

Predicting Inductance Roll Off with DC Excitations

Jennifer D. Pollock, Weyman Lundquist and Charles R. Sullivan
Thayer School of Engineering at Dartmouth, Hanover, NH 03755, USA
West Coast Magnetics, Stockton CA 95215

Email: jennap@ieee.org, WLundquist@wcmagnetics.com and charles.r.sullivan@dartmouth.edu
Website: www.power.thayer.dartmouth.edu and www.wcmagnetics.com

Abstract—The ability to predict how the inductance of an inductor will change with applied dc current is investigated for several different magnetic core materials. The goal of this work is to develop a method that will allow this constraint to be incorporated into the optimization of an inductor for power conversion applications. Theoretical predictions of an inductor’s saturation characteristics are compared to the measured performance. A method to predict the saturation of an inductor is presented as well as methods for adjusting the prediction considering measured material behavior.

I. INTRODUCTION

The design of an inductor for power conversion applications requires tradeoffs to be made between component size, cost and efficiency. In order to optimize these tradeoffs for a particular application, an accurate model of a component’s performance is needed. Accurate models for winding loss [1]-[7] and core loss [8]-[16] have been developed, but models to predict how the inductance of a power inductor rolls off with applied dc current are still quite basic. A simple design approach is to calculate the number of turns needed to maintain the required inductance at some maximum dc current for a given core size and saturation flux density. The challenge here is to know the flux density at which the inductance drops to an unacceptable level.

Core manufacturers supply a range of data about a core’s behavior under a variety of conditions, including temperature, frequency and magnetic field strength. However, it can be difficult to combine this information to reflect the operating conditions and core configurations commonly found in inductors for power conversion applications. Although a manufacturer typically provides a full BH loop, it is usually a full loop measured on a closed core without dc bias. Applying this data to a component with air gaps in the magnetic path and an excitation composed of a dc current with some ac ripple riding on it is not straightforward and can lead to errors in a prediction of saturation characteristics. Even when the manufacturer provides data on permeability roll-off with DC bias, additional analysis is required to apply this to a gapped core.

Consider the BH loops shown in Fig. 1. One way to estimate the permeability of a material is to sketch a

centerline in the BH loop as done in Fig. 1 and estimate the permeability as the slope of that curve. When a dc current is present, the BH loop is shifted and no longer is centered around zero. Any ripple current present will create a loop around this point, known as a minor loop, as shown in Fig. 1. When the slope of the centerline of the minor loop is compared to the slope of the centerline of the full loop, it is clear that the material behaves differently under these operating conditions.

This work investigates how to use the available data and/or simple measurements to determine the saturation characteristics of several different magnetic materials used in inductors for power conversion applications. First, a general method to theoretically predict the saturation of an inductor is presented in Section II. Step-by-step instructions to apply this method using a material’s magnetic properties are provided in Section III. The experimental setup used to measure the test inductors is described in Section IV. A BH curve is extracted from the measured inductance and DC current data in Section VI. This BH curve is then used to predict an inductor’s saturation under DC bias. The conclusions are discussed in Section VII.

II. THEORETICAL CALCULATION OF INDUCTANCE VARIATION UNDER DC BIAS

In this section, we derive the inductance of a component from a theoretical point of view. Because the goal of this work is to optimize the design of power inductors, we are interested in a method to include in the design process. While the method itself is straightforward, care is needed to correctly use an appropriate characterization material properties, and to account for any air gaps in the magnetic path.

We first consider a simplified ideal case in which the core material is described by a single-value, non-hysteric BH curve. This is the case in which the axis of the minor loop is parallel to the centerline of the major loop, contrary to the more realistic case shown in Fig. 1. Our goal is to plot a curve of inductance as a function of dc current. However, rather than solving for inductance at a given dc current, we instead start with a value of magnetic field, H , and solve for

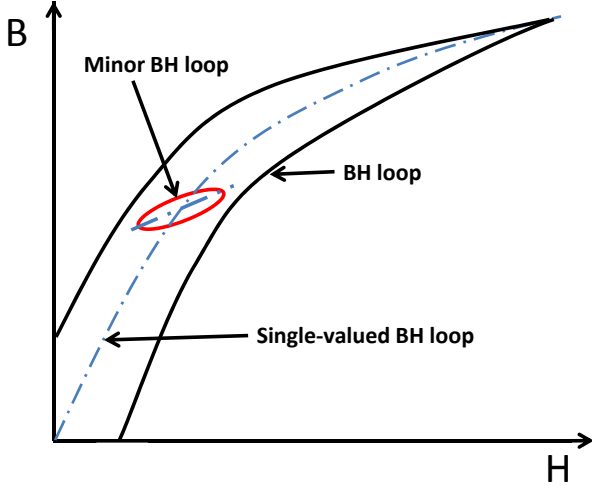


Fig. 1. A schematic showing a typical BH curve with a dashed centerline. A minor loop with DC bias is also shown. The slope of the axis of the minor loop is the small-signal permeability needed to determine the inductance at this bias point.” Note that this is not parallel to the slope of the major loop.

both dc current and inductance at that operating point. This approach avoids complications in solving for the operating point on the BH curve when the BH curve data is only available in tabular form.

To find the dc current as a function of magnetic field, H , the magnetomotive force dropped across the core reluctance and air gap reluctance are determined. Given tabular BH curve data, the flux density, B , can be looked up at a specified dc field H_{dc} . The flux in a core, Φ , is found from $\Phi = B(H_{dc}) \cdot A_{core}$ assuming the flux density is uniform across the core area, A_{core} . The magnetomotive force dropped across any air gap in the magnetic path is

$$MMF_{gap}(H_{dc}) = \Phi(H_{dc})\mathcal{R}_{gap} \quad (1)$$

where \mathcal{R}_{gap} is the reluctance of the gap.

The magnetomotive force dropped across the core is

$$MMF_{core}(H_{dc}) = H_{dc}\ell_{core} \quad (2)$$

where ℓ_{core} is the effective length of the core. The dc current is calculated at H_{dc} considering a specific number of turns, N

$$I_{dc}(H_{dc}) = \frac{MMF_{gap}(H_{dc}) + MMF_{core}(H_{dc})}{N}. \quad (3)$$

To calculate the inductance, we need the relative permeability, $\mu_r(H_{dc})$, of the core. For a single-valued BH curve, μ_r is

$$\mu_r(H_{dc}) = \frac{1}{\mu_0} \left. \frac{\partial B}{\partial H} \right|_{H_{dc}}. \quad (4)$$

The core reluctance, $\mathcal{R}_{core}(H)$ is

$$\mathcal{R}_{core}(H_{dc}) = \frac{\ell_{core}}{\mu_0 \mu_r(H_{dc}) A_{core}}. \quad (5)$$

The inductance can then be determined

$$L(H_{dc}) = \frac{N^2}{\mathcal{R}_{gap} + \mathcal{R}_{core}}. \quad (6)$$

In practice, we have not found any material for which the simplified method is accurate, which indicates that the slope of the minor loops is, as shown in Fig. 1, different from the slope of the major loop. Thus, we now consider the case that includes the behavior with minor loops and we again find the inductance and dc current for a range of H_{dc} . In addition to the same data that is required above, we also need information on how the relative permeability changes with dc magnetic field strength.

The relative permeability of a minor loop, $\mu_{core,m}$, is used to determine a core reluctance, $\mathcal{R}_{core,m}(H)$

$$\mathcal{R}_{core,m}(H) = \frac{\ell_{core}}{\mu_0 \mu_{core,m}(H) A_{core}}. \quad (7)$$

The inductance then becomes

$$L(I_{dc}) = \frac{N^2}{\mathcal{R}_{gap} + \mathcal{R}_{core,m}}. \quad (8)$$

A plot the inductance verses dc current can now be generated from Eqs. (8) and (3).

III. PROCEDURE TO PREDICT INDUCTANCE VARIATION UNDER DC BIAS

To use the method presented in Section II, it is necessary to gather information on the inductor size, number of turns and core material properties. Ideally we would want a single-valued BH curve that describe the material behavior under dc bias. However, the data comes in a variety of forms. For the powdered metal material considered here, the information given was an initial material permeability and a curve describing how the permeability changes with applied dc magnetic field. This information can be used to find the relative permeability of the core but a BH curve is still needed to find the flux density at that field for the gap reluctance. For the ferrite material considered, the relative permeability of the core was determined from the reversible permeability curve and the flux density was found from the BH curve. The difference between the relative permeability given by the BH curve and the reversible permeability curve is shown in Fig. 9. This demonstrates the how the measurement conditions affect material properties. To accurately predict and inductor performance, the operating conditions use to characterize the material should match the operating conditions.

The method requires a gap length to be specified. This gap reluctance is determined by the required inductance. The inductance can be calculated for a design or measured on an existing inductor. The gap reluctance needed to meet the inductance specification

The gap reluctance is found from the inductance by

$$\mathcal{R}_{gap} = \frac{N^2}{L} - R_{core} \quad (9)$$

IV. EXPERIMENTAL SETUP

The circuit shown in Fig. 2 was built to test a series of the prototype inductors, represented by DUT_1 and DUT_2 . The inductance was measured by an Agilent 4294A impedance analyzer and represented the parallel combination of DUT_1 and DUT_2 , which were built to be identical. A switch was used to protect the impedance analyzer while the dc current setting was changed. Capacitors C_1 and C_2 were very large electrolytic capacitors.

Some commercial impedance analyzers have DC bias current capability built-in, or available as an internal or external option. The advantages of such a system over the configuration shown in Fig. 2 include the fact that only one inductor is needed for testing, and typically the ability to automatically sweep and gather data without programming an external controller. However, such instruments are limited in frequency range and current capability, whereas a setup as shown in Fig. 2 can be configured for any necessary current and frequency range for only the cost of a power supply with the necessary current capability, and the cost of building two test inductors. It is also possible to set up a configuration like that in Fig. 2, but with one reference inductor with known saturation characteristics, preferably not saturating significantly in the range of interest, and one inductor to be measured. To identical reference inductors are normally needed so that they can be characterized as shown in Fig. 2 prior to use. They may then be optionally configured in parallel when used for the characterization of other inductors, in order to double the current available before they saturate.

The specifications for the prototype inductors are listed in Table I and a picture of prototype #1 is shown in Fig. 3. The measured results for an inductor are shown in Figs. 4, 5, 6, 7 and 8 for Micrometals -26 material, Micrometals -52 material, Kool Mu material and Ferroxcube 3C90 material. The performance of each inductor was measured for several different air gap lengths.

V. COMPARISON OF MEASURED AND PREDICTED INDUCTANCE

A method to calculate the roll-off of any particular inductor was given in Section II. However, it is often

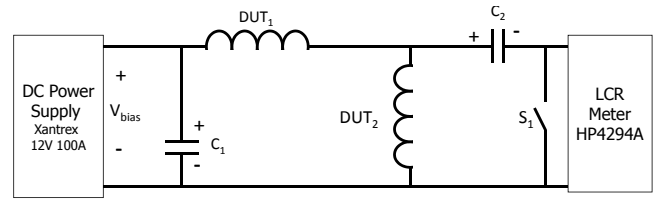


Fig. 2. The test setup used to measure the saturation of the inductors.

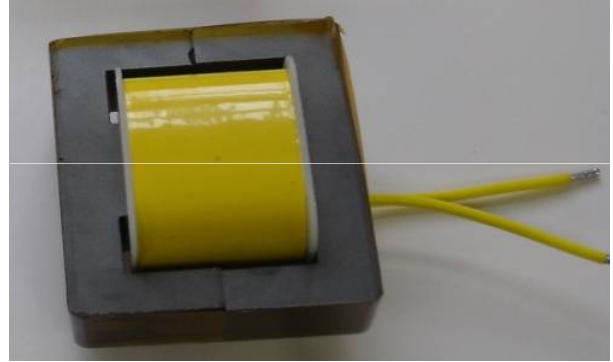


Fig. 3. A prototype inductor.

TABLE I
INDUCTOR SPECIFICATIONS

Parameter	Prototype 1	Prototype 2	Units
Core Size	EI225	E54/24/19	NA
Effective core area, A_{core}	3.58×10^{-4}	3.37×10^{-4}	m^2
Effective core length, ℓ_{core}	115	107	mm
Number of turns, N	30	30	NA
Winding Type	Foil	Wire	NA

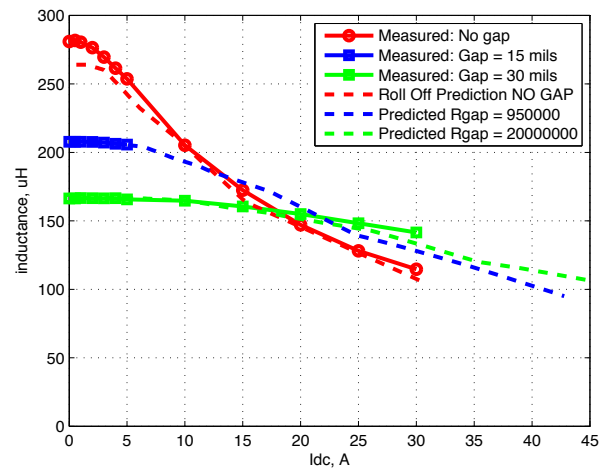


Fig. 4. The measured inductance is compared to the predicted inductance roll-off for the Micrometals -26 material in prototype #1.

necessary to modify this depending on the information provided by the manufacturer.

As shown in Fig. 4, the measured saturation for Micrometals -26 material matches the predicted saturation very well for all three air gap lengths considered. For this particular material, the measured inductance with no air gap is about 6% higher than the predicted inductance. This is within the allowable 10% variation specified on the data sheet.

The results for the Micrometals -52 material were barely within plus or minus 10% of the predicted values as shown in Figs. 5 and 6. In this case, the measured inductance was larger than predicted over the entire range considered. This means that the measured relative permeability is larger than the permeability given on the data sheet. This result indicates that more material has been packed into the core so there are more particles of iron which contributes to the increased permeability.

As shown in Fig. 7, the measured saturation for Magnetics Kool Mu 60 permeability material matches the predicted saturation very well for the air gap lengths considered. Again, we see the measured unloaded inductance higher than predicted by the given initial permeability, but the results are within the variation specified by the manufacturer.

The results for a ferrite material, 3C90, are shown in Fig. 8 where the measured inductance drops off before the predicted behavior. The predicted performance matched the measured results for both gapped configurations with the 20% range until the inductance dropped below 25% of the unloaded value. We believe that the faster roll-off in our experiments may be due to heating of the core from winding loss during the measurement.

VI. MEASURING MATERIAL PROPERTIES

Often, magnetic material data sheets do not include both of the pieces of information needed to predict inductance rolloff: small-signal permeability as a function of field strength, and a dc BH curve. Thus, measurements are often needed. It is straightforward to use impedance measurements to find a permeability curve, as described below in Section VI-A. The most straightforward approach to measuring a BH curve is to set up an inductive BH loop tracing apparatus or use a commercial instrument for that purpose. However, it is also possible to combine two measurements of impedance with DC bias to extract a BH loop. Given that the same apparatus is required for measuring permeability as a function of bias, this approach is likely to be more convenient, and is described and demonstrated in Section VI-B.

Even when the necessary data are provided on the magnetic material datasheet, it may be desirable to make

measurements as described below. In some cases, it may be important to collect measurements at different temperatures, and the measurements will inherently include any effects of core shape and flux crowding. In addition, the datasheet often provides information in graphical form, requiring the user to automatically or manually convert it to numerical data before it can be used in calculations.

A. Measuring Permeability

Small-signal permeability as a function of dc bias can be measured with an impedance analyzer configured for dc bias as discussed in Section IV. On an un-gapped core, the dc magnetic bias field H_{dc} applied by a bias current I_{dc} is simply

$$H_{dc} = \frac{NI_{dc}}{\ell_{eff}} \quad (10)$$

and the relative permeability is

$$\mu_r(H_{dc}) = \frac{\ell_{eff}L(I_{dc})}{\mu_0 A_{eff} N^2} \quad (11)$$

Both of the equations above assume no gap. In practice, when a two-piece core is assembled with no deliberate gap, there may be a small effective gap due to imperfect mating of the surfaces. Clean surfaces tightly clamped together should minimize this problem, and if this gap is negligible compared to the gap to be used in practice, the effect on the measured curves is not important. However, in case it is not possible to assemble the core with a sufficiently small gap (for example, if the only cores available have a gapped center leg), it is also possible to extract permeability from measurements made with a gap, if a BH curve is available. The BH curve could be from the manufacturer or from the measurement approach discussed in the next section. A disadvantage of extracting the permeability from a gapped measurement is that it requires assuming a known initial small-signal permeability at zero bias. Thus, when possible, it is better to measure an ungapped core, with clean, tightly mated surfaces. However, when necessary, the procedure described below can be used.

To extract permeability from the inductance measurements on a gapped core, one must know the reluctance of the gap. This can be calculated from the zero-bias inductance measurement assuming that the core reluctance under zero bias can be accurately calculated from the datasheet value of initial permeability.

$$\mathcal{R}_{gap} = \frac{N^2}{L(I_{dc} = 0)} - \mathcal{R}_{core}(I_{dc} = 0). \quad (12)$$

One can then find the core reluctance at varying bias levels by subtracting this fixed gap reluctance from the total

reluctance calculated from the measured inductance.

$$\mathcal{R}_{core}(I_{dc}) = \frac{N^2}{L(I_{dc})} - \mathcal{R}_{gap}. \quad (13)$$

Because we rely on the assumption that the gap reluctance is fixed, it is important that the core be tightly clamped together, such that the gap length does not vary as the dc bias increases, and the magnetic force compressing the gap increases. The relative permeability can be calculated from this core reluctance

$$\mu_r(I_{dc}) = \frac{\ell_{eff}}{\mu_0 A_{eff} \mathcal{R}_{core}(I_{dc})}. \quad (14)$$

To convert this relative permeability as a function of current, which is only valid for the particular gap at which it was measured, into relative permeability as a function of bias field H_{dc} , one can apply (??) and (??) to find the relationship between current and bias field.

B. Extracting a BH Curve from Impedance Measurements

It is possible to solve for the nonlinear relationship between B_{dc} and H_{dc} from two sets of two impedance measurements, each with a different gap length, and each over a range of dc bias currents. From each measurement, we can easily solve for the core reluctance as described above (13), and if we find dc bias levels for each gap length that result in the same core reluctance (and thus the same relative permeability), we know that those different bias levels result in the same operating point on the BH curve for each of the two gap lengths. We can then derive two equations—one for each gap length—that we can solve for the two unknowns, B_{dc} and H_{dc} .

If one of the two sets of measurements is with a ungapped core, the magnetic field bias H_{dc} can be directly obtained from the DC bias current (10). If the other measurement is made with a gap large enough that the reluctance of the gap is much larger than the reluctance of the core, there is approximately a simple linear relationship between the applied current and the flux and flux density in the core. When one matches up a pair of measurements from each set that have the same core reluctance, one then can obtain H_{dc} from the current in the ungapped test, and B_{dc} from the current in the large-gap test, thus obtaining one point on the BH curve.

In practice, making one measurement on an ungapped core is practical and effective, but the gap used in the other measurement should not be extremely large, because if the gap reluctance is much greater than the core reluctance, it becomes difficult to measure the core reluctance accurately. Thus, it is best to make this measurement with the magnitude of the gap reluctance similar to the magnitude of the

core reluctance. It is then necessary to solve algebraically for the magnetic flux in this measurement rather than obtaining it directly from the current and the gap reluctance. Over the range of bias values tested, the core reluctance can vary over several orders of magnitude. For best accuracy in determining a BH curve, one might consider using different gaps in different ranges of bias, but in practice any gap length on the same order as the gap lengths to be used in practical designs will give adequate precision for predicting inductance rolloff.

Although we obtained the best results by using one set of measurements on an ungapped core and set one measurements on a gapped core, the equations are similar for the case of using two different gap lengths in the two different tests. If, as we recommend, one of the measurement sets is made with an ungapped core, the gap reluctance for that set of measurements is simply zero.

For each of the two measurements sets, the relative permeability is calculated from (12), (13), and (14). Corresponding points with the same relative permeability are matched up on the two curves. We then have two current values, $I_{dc,g1}$ and $I_{dc,g2}$ that correspond to the same B_{dc} and H_{dc} values, but with different gap lengths. By writing the DC magnetic circuit equations for each, we obtain two equations in the two unknowns, B_{dc} and H_{dc} . These two equations can both be written

$$I_{dc,i}N = B_{dc}A_{eff}\mathcal{R}_{gap,i} + H_{dc}\ell_{eff} \quad (15)$$

where $I_{dc,i}$ and $\mathcal{R}_{gap,i}$ use the index i to indicate the different values for the measurements with different gap lengths. To solve these simultaneous equations, one can equate $H_{dc}\ell_{eff}$ in each to obtain

$$(I_{dc,1}N - B_{dc}A_{eff}\mathcal{R}_{gap,1}) = (I_{dc,2}N - B_{dc}A_{eff}\mathcal{R}_{gap,2}) \quad (16)$$

leading to

$$B_{dc} = \frac{(I_{dc,2} - I_{dc,1})N}{A_{eff}(\mathcal{R}_{gap,2} - \mathcal{R}_{gap,1})} \quad (17)$$

H_{dc} can then be found by substituting B_{dc} into (15)

$$H_{dc} = \frac{1}{\ell_{eff}} (I_{dc,i}N - B_{dc}A_{eff}\mathcal{R}_{gap,i}) \quad (18)$$

preferably using the smaller- or zero-gap values of $I_{dc,i}$ and $\mathcal{R}_{gap,i}$, such that the subtraction does not magnify error.

The results of extracting a BH curve by this method from measurements with no gap and with a 0.76 mm gap are shown in Fig. 10. The measurements on the ungapped core of Ferroxcube 3C90 material were performed both starting at zero bias current, ramping up to 4 A, and starting at 4 A ramping down to zero, resulting in the two branches of a

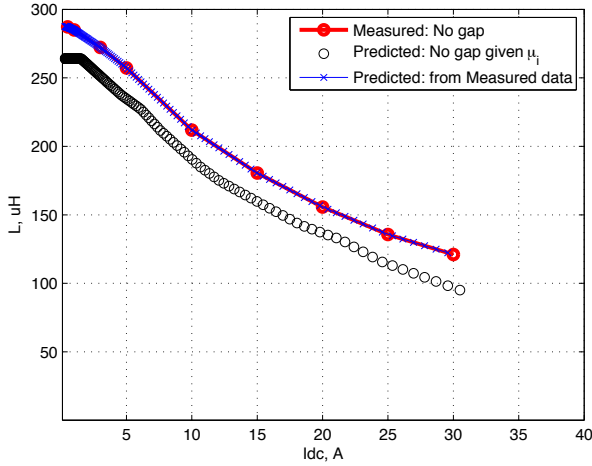


Fig. 5. The measured and predicted inductance saturation are compared for the inductors with no air gap in the core using Micrometals -52 material in prototype #1.

hysteresis loop shown. The results are compared to points transcribed by hand from the datasheet BH curve. Although the agreement is generally good, the experimental results show a more rounded shape, and a lower saturation value. These may be at least in part a result of flux crowding in the corners of the E core, leading these regions to saturate earlier.

The experimental BH and permeability curves were then used to predict rolloff with two different gap lengths as shown in Fig. ???. Because the data was derived from the data for the 0.76 mm gap, this curve lines up perfectly with the experimental results. More noteworthy is that the data for the 0.38 mm gap also lines up very well, indicating that the method works very well for predicting what happens with a different gap length than the size used for characterizing the core.

VII. CONCLUSION

The saturation characteristics of an inductor are an important aspect to consider when optimizing an inductor design. The ability to accurately predict the saturation characteristic is highly desirable and requires the correct information about a material's performance with the core configurations and excitation commonly found in power inductors. The method presented here works well to predicted the behavior and has been experimentally verified. The core materials considered here demonstrate some of the challenges in determining the saturation characteristics of a particular inductor using data from the material data sheet.

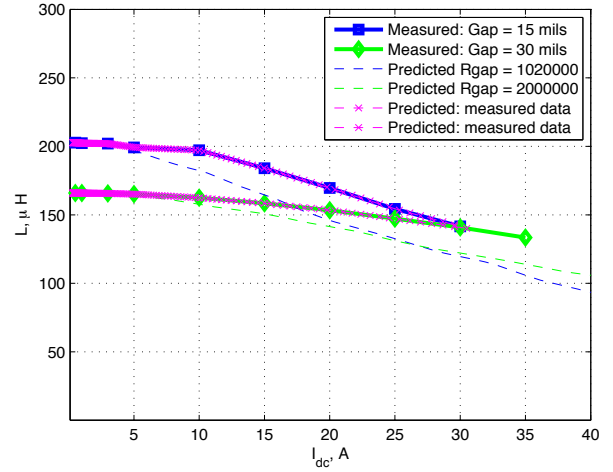


Fig. 6. The measured and predicted saturation are compared for the inductors with air gaps in the core using Micrometals -52 material in prototype #1.

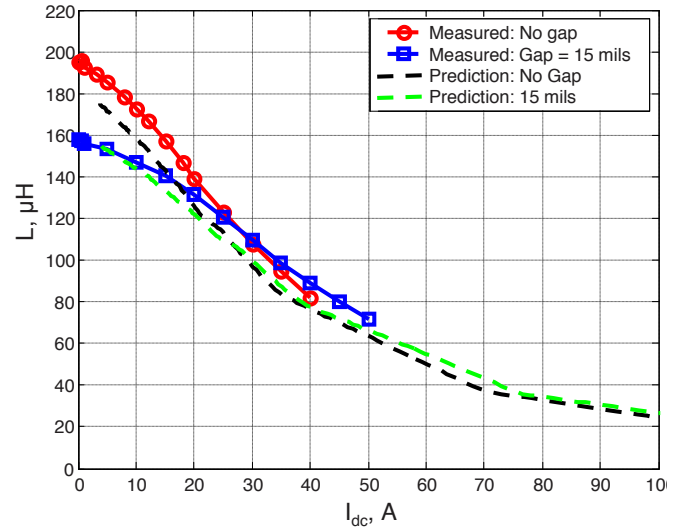


Fig. 7. The measured inductance is compared to the predicted inductance roll-off for the 60 permeability Kool Mu material in prototype #2.

REFERENCES

- [1] C. R. Sullivan, "Optimal choice for number of strands in a litz-wire transformer winding," *IEEE Transactions on Power Electronics*, vol. 14, no. 2, pp. 283–291, 1999.
- [2] P. Dowell, "Effects of eddy currents in transformer windings," *Proceedings of the IEE*, vol. 113, no. 8, pp. 1387–1394, Aug. 1966.
- [3] V. Van den Bossche, A.; Valchev, "Eddy current losses and inductance of gapped foil inductors," in *IEEE 28th Annual Conference of the Industrial Electronics Society*, 2002, pp. 1190–1195.
- [4] G. R. Skutt and P. S. Venkatraman, "Analysis and measurement of high-frequency effects in high-current transformers," in *APEC '90. Fifth Annual Applied Power Electronics Conference and Exposition*, 1990, pp. 354–64.
- [5] M. P. Perry, "Multiple layer series connected winding design for minimum loss," *IEEE Transactions on Power Apparatus and Systems*, pp. 116–123, 1979.

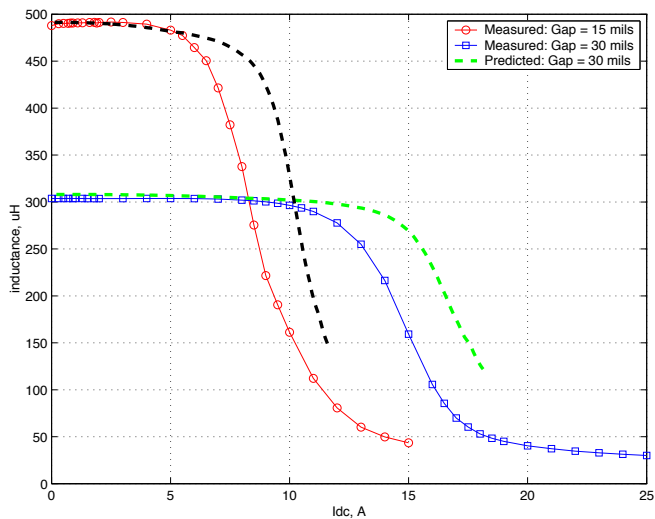


Fig. 8. The measured saturation is compared to the predicted roll-off for the ferrite material 3C90 in prototype #2.

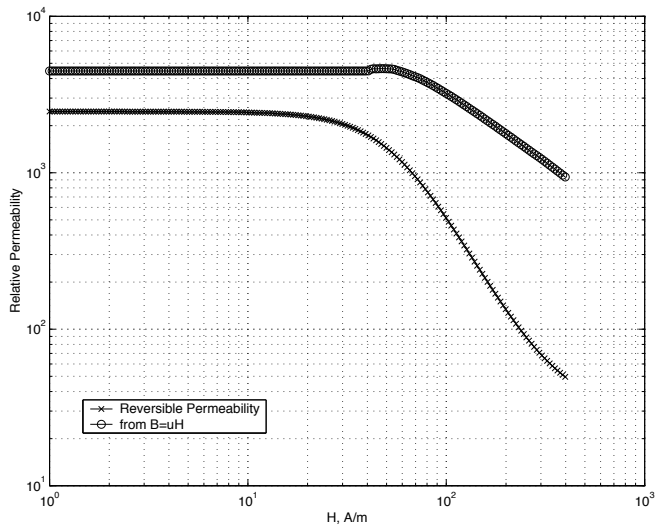


Fig. 9. Two different relative permeability curves from the ferrite material 3C90. The lower curve is the reversible permeability curve and the upper curve is determined using Eq. (4) and the centerline of the given BH loop.

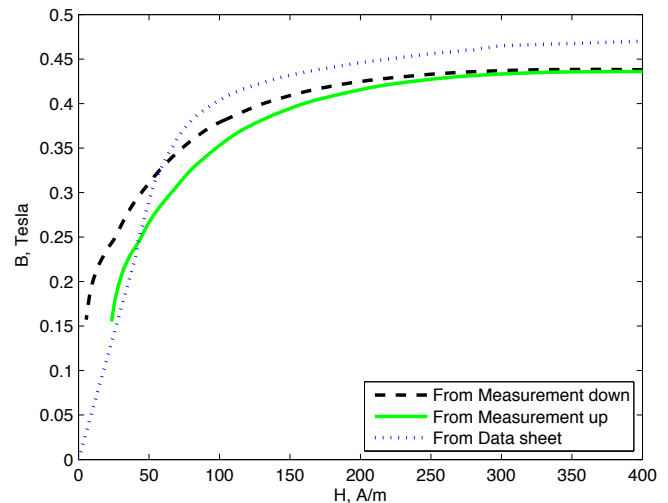


Fig. 10. A BH curve is extracted from the measured inductance and DC current data. It shows the difference between the behavior of the material under dc bias and the operating conditions of the data sheet BH loop data.

[6] F. J. Odendaal W.G. and C. W.A., "Combined numeric and analytic methods for foil winding design," in *Proceedings of PESC 1994 - Power Electronics Specialists Conference*, vol. 2, 1994, pp. 843–849.

[7] P. Wallmeier, "Improved analytical modeling of conductive losses in gapped high-frequency inductors," *IEEE Transactions on Industry Applications*, vol. 37, no. 4, pp. 1045–54, July-Aug. 2001.

[8] J. Li, T. Abdallah, and C. R. Sullivan, "Improved calculation of core loss with nonsinusoidal waveforms," in *Conference Record of the 2001 IEEE Industry Applications Conference. 36th IAS Annual Meeting*, 2001, pp. 2203–2210.

[9] K. Venkatachalam, C. R. Sullivan, T. Abdallah, and H. Tacca, "Accurate prediction of ferrite core loss with nonsinusoidal waveforms using only Steinmetz parameters," in *COMPEL 2002: 8th IEEE*

Workshop on Computers in Power Electronics, 2002.

[10] B. A. Reinert, J. and R. De Doncker, "Calculation of losses in ferro- and ferrimagnetic materials based on the modified steinmetz equation," in *34th Annual IEEE Industrial Application Society Conference*, 1999, pp. 2087–92.

[11] A. Brockmeyer and J. Paulus-Neues, "Frequency dependence of the ferrite-loss increase caused by premagnetization," in *Proceedings of 1997 IEEE Applied Power Electronics Conference and Exposition - APEC'97*, 1997, pp. 375–80.

[12] D. T. Albach, M. and A. Brockmeyer, "Calculating core losses in transformers for arbitrary magnetizing currents a comparison of different approaches," in *Proceedings of PESC 1996 - Power Electronics Specialists Conference*, vol. 2, 1996, pp. 1463 – 1468.

[13] H. Saotome and Y. Sakaki, "Iron loss analysis of Mn-Zn ferrite cores," in *IEEE Transactions on Magnetics*, no. 1, 1997, pp. 728–34.

[14] K. H. Carpenter, "Simple models for dynamic hysteresis which add frequency-dependent losses to static models," in *IEEE Transactions on Magnetics*, no. 3, 1998, pp. 619–22.

[15] J.-T. Hsu and K. Ngo, "A hammerstein-based dynamic model for hysteresis phenomenon," in *IEEE Transactions on Power Electronics*, no. 3, 1997, pp. 406–413.

[16] G. Bertotti, "General properties of power losses in soft ferromagnetic materials," in *IEEE Transactions on Magnetics*, no. 1, 1988, pp. 621–630.